

CeNiAsO: an antiferromagnetic dense Kondo lattice

Yongkang Luo¹, Han Han¹, Hao Tan¹, Xiao Lin¹, Yuke Li¹,
Shuai Jiang¹, Chunmu Feng¹, Jianhui Dai¹, Guanghan Cao^{1,2},
Zhu'an Xu^{1,2}, and Shiyan Li³

¹ Department of Physics, Zhejiang University, Hangzhou 310027, P. R. China

² State Key Laboratory of Silicon Materials, Zhejiang University, Hangzhou 310027, P. R. China

³ Department of Physics and Laboratory of Advanced Materials, Fudan University, Shanghai 200433, P. R. China

E-mail: zhuan@zju.edu.cn

Abstract. A cerium containing pnictide, CeNiAsO, crystallized in the ZrCuSiAs type structure, has been investigated by measuring transport and magnetic properties, as well as specific heat. We found that CeNiAsO is an antiferromagnetic dense Kondo lattice metallic compound with Kondo scale $T_K \sim 15$ K and shows an enhanced Sommerfeld coefficient of $\gamma_0 \sim 203$ mJ/mol·K². While no superconductivity can be observed down to 30 mK, Ce ions exhibit two successive antiferromagnetic (AFM) transitions. We propose that the magnetic moment of Ce ion could align in the G type AFM order below the first transition at $T_{N1}=9.3$ K, and it might be modified into the C type AFM order below a lower transition at $T_{N2}=7.3$ K. Our results indicate that the $3d-4f$ interlayer Kondo interactions play an important role in Ni-based Ce-containing pnictide.

PACS numbers: 74.70.Dd, 75.20.Hr, 74.62.Bf

1. Introduction

The discovery of iron-based arsenide superconductor LaFeAsO_{1-y}F_y[1] has triggered enormous enthusiasm in searching new high transition temperature (T_c) superconductors in Fe or Ni-based pnictides[2, 3, 4, 5, 6]. T_c has been raised up to above 50 K when La is replaced by other rare earth elements in the so-called 1111 type family [7, 8]. The parent compound of the 1111 type pnictides, $LnTPnO$ (Ln = rare earths, T = transition metals, Pn = As, P), is of the prototype of ZrCuSiAs structure, where the conducting TPn layer is sandwiched by the insulating LnO layer. So far superconductivity (SC) can be induced in the Fe(Ni)As-based pnictides by many different ways of chemical doping or by applying high pressure.

Among all these $LnTPnO$'s, the members $Ln = Ce$ show extremely interesting electronic properties. CeFeAsO, as a prototype parent compound of Fe-based superconductor, is an itinerant bad metal. A spin-density-wave(SDW)-like antiferromagnetic (AFM) transition of d electrons was observed around ~ 140 K, and the AFM transition of the Ce³⁺ local moments was observed below 4 K [9]. SC has been induced by electron doping (i.e. F-for-O doping) when the SDW long range order of the Fe $3d$ -electrons is suppressed[3]. On the other hand, CeFePO is a paramagnetic (PM) heavy-fermion (HF) system which is near the ferromagnetic (FM) instability[10, 11]. By comparison, CeOsPO shows the Ce³⁺ AFM order at 4.5 K while CeRuPO is a rare example of the FM Kondo lattice with $T_C = 15$ K[12]. For the case of $T = Co$, both CeCoPO and CeCoAsO show the FM correlated Co- $3d$ magnetism[13, 14, 15].

It is noted that the nickel arsenide LaNiAsO is a low T_c superconductor and T_c can be enhanced upon F-doping [5, 6]. Interestingly, the partial substitution of Fe by Ni in LaFeAsO, which introduces two more $3d$ electrons by each Ni²⁺ dopant, can induce SC in a very narrow doping regime [16]. Moreover, the normal state resistivity shows an upturn behavior at low temperatures, suggesting a possible Kondo-effect induced semiconductor behavior. However, there are very few reports on the physical properties of 1111 type NiAs-based pnictides other than LaNiAsO. The early report did not observe SC above 2 K and suggested a suspicious FM order in CeNiAsO [17], although its structure and the valence of Ce ion has been studied [18].

In this paper, we report the systematic investigation on the physical properties of CeNiAsO. No evidence of SC is observed for temperature down to 30 mK. While there is no local magnetic moment on Ni ions, two successive antiferromagnetic transitions related to Ce ions are observed. We propose that the Ce moments could align in "G" type AFM order first at $T_{N1} = 9.3$ K, and then transform into "C" type at a lower temperature $T_{N2} = 7.3$ K. The Sommerfeld coefficient is about 203 mJ/mol·K², indicating that CeNiAsO is an enhanced correlated Kondo lattice compound. All these results imply a strong hybridization between $4f$ - and $3d$ -electrons and highlight the important role of the $3d$ - $4f$ interlayer Kondo physics in nickel based cerium containing pnictide.

2. Experimental

Poly-crystalline CeNiAsO sample of high purity was synthesized by solid state reaction. Ce, Ni, As, and CeO₂ of high purity ($\geq 99.95\%$) were used as starting materials. Firstly, CeAs was presynthesized by reacting Ce discs and As powders at 1320 K for 72 h. NiAs was presynthesized by reacting Ni and As powders at 970 K for 20 h. Secondly, powders of CeAs, CeO₂, Ni, and NiAs were weighted according to the stoichiometric ratio, thoroughly ground, and pressed into a pellet under a pressure of 600 MPa in an Argon filled glove box. The pellet was packed in an alumina crucible and sealed into an evacuated quartz tube, which was then slowly heated to 1450 K and kept at that temperature for 40 h. For comparison, polycrystalline sample of LaNiAsO was also synthesized, in the similar process, where La₂O₃ was used as the oxygen source.

Powder X-ray diffraction (XRD) was performed at room temperature using a D/Max-rA diffractometer with Cu-K α radiation and a graphite monochromator. Lattice parameters were derived by Rietveld refinement using the programme RIETAN 2000 [19]. X-ray Photoelectron Spectrum (XPS) analysis was carried out by using a VG ESCALAB MARK II device with Mg-K α ($h\nu = 1253.6$ eV) nonmonochromatized source operating in Constant Analysis Energy (CAE, 50 eV) mode, and data were collected in a step of 0.2 eV. Before taking the XPS data, the CeNiAsO sample was pre-polished by the argon beam in the vacuum to make a newly polished sample surface. Electrical resistivity was measured with a standard four-probe method in a Quantum Design physical property measurement system (PPMS-9, for $T \geq 2$ K) and a dilution refrigerator (for $T < 2$ K), while Hall coefficient was measured by scanning field from -5 T to 5 T. Thermopower was measured by a steady-state technique and a pair of differential type E thermocouples was used to measure the temperature gradient. Specific heat was measured by heat pulse relaxation method in PPMS-9. The dc magnetization measurement was carried out in a Quantum Design magnetic property measurement system (MPMS-5) in zero-field-cooling (ZFC) and field-cooling (FC) protocols under a magnetic field H of 1000 Oe.

3. Results and discussion

Fig. 1 shows Rietveld refinement of XRD patterns of CeNiAsO. All the XRD peaks can be well indexed in to the tetragonal ZrCuSiAs-type structure with P4/ nmm (No.129) space group, and no obvious impurity trace can be found. The quality factor (χ^2) of this refinement reaches to as low as 0.88, guaranteeing the goodness of sample quality. The refined structural parameters are listed in Tab. 1 with a comparison to CeFeAsO, from which we can find that CeNiAsO has a slightly longer a -axis but much shorter c -axis compared to its iron based counterpart. Because arsenic is drawn closer to the Ni plane, the thickness of NiAs layer, d_{NiAs} , is much smaller than d_{FeAs} , while the angle of As-T-As ($T = \text{Fe or Ni}$, see the inset of Fig. 1) is enlarged.

Fig. 2 shows temperature dependence of dc magnetic susceptibility of CeNiAsO

measured under $H = 1000$ Oe. The data above 150 K exhibit good Curie-Weiss behavior, and can be well fitted to $\chi = \chi_0 + C/(T - \theta_W)$, with χ_0 being the temperature independent item, and θ_W the Weiss temperature. The fitting reports that $\theta_W = -31.8$ K. The obtained effective moment $\mu_{eff} = 2.24 \mu_B$ is slightly smaller than that of a free Ce^{3+} ion, $2.54 \mu_B$. For $T < 100$ K, we observed a change in the slope of the temperature dependence of inverse susceptibility (right axis of Fig. 2), and the fitting parameters are $\mu_{eff} = 2.16 \mu_B$, $\theta_W = -25.6$ K. The change in the slope should be ascribed to the crystal electric field (CEF) effect. It has been demonstrated both theoretically and experimentally that Ni ions do not exhibit magnetic ordering in the nickel based pnictides[6, 20, 21, 22, 23]. Therefore, the Curie-Weiss analysis suggests that the observed effective moments in CeNiAsO should come from Ce ions. When cooled to low temperature, a peak in susceptibility is observed around 9.3 K, followed by an upturn when further cooled. Since the Weiss temperature derived from the Curie-Weiss analysis is negative, it is reasonable to conclude that Ce moments are ordered antiferromagnetically below 9.3 K. The AFM ordering of Ce ions is compatible with the linear field dependence of magnetization (data not shown here), as well as the small magnitude of susceptibility in comparison with CeFeAsO [11].

One possible interpretation to the noticeable deviation of the obtained effective moment from that of the free Ce^{3+} ion is the presence of valence state Ce^{4+} which has no $4f$ -electron and local moment. To investigate the valence of Ce in this compound, we thus carried out the XPS experiment. The XPS spectrum of CeNiAsO is shown in Fig. 3. After subtracting the background, the XPS spectrum can be well fitted by a combination of ten Gaussian peaks, i.e., $\text{Ce(III)} = v^0 + v' + u^0 + u'$, and $\text{Ce(IV)} = v + v'' + v''' + u + u'' + u'''$, with u and v corresponding to the spin-orbit split $3d_{3/2}$ and $3d_{5/2}$ core holes, respectively. The positions of these peaks are taken from Ref.[24], where XPS spectrum of CePO_4 (Ce^{3+}) and CeO_2 (Ce^{4+}) were presented. We found that Ce^{3+} is dominant in CeNiAsO, but there is a small trace of Ce^{4+} which should account for the small peak around 916 eV [25]. An early report on the Ce $3d$ XPS and Ce L_3 -edge XANES analysis of CeNiAsO and CeFeAsO by Balnchard et al suggested that the valence of Ce should be close to $3+$ [18]. In other Ce containing compounds with strong Kondo interaction, for example, in CePd_2Al_3 [26], it is common that Ce has a valence very close to $3+$. Therefore, although the valence effect may play some role in the reduction of effective magnetic moment of Ce, a more likely interpretation to this reduction could mainly come from the CEF effect, which will be discussed hereinafter.

The transport properties of CeNiAsO are presented in Fig. 4. The resistivity exhibits several prominent features. Firstly, the magnitude of resistivity at room temperature, i.e., ρ_{300K} , has a small value of $3.9 \mu\Omega\cdot\text{m}$, which is about two orders of magnitude smaller than that of CeFeAsO (see in Tab. 1). The good metallicity of CeNiAsO can be also confirmed by Hall coefficient R_H measurement, as shown in the lower inset. R_H remains as a nearly temperature independent constant above 150 K, and converges to $0.68 \times 10^{-4} \text{cm}^3/\text{C}$. A rough estimate from single band model leads to a carrier density of $\sim 10^{24} \text{cm}^{-3}$, which is an upper limit of charge carrier density in a multi-

band system, about 3 orders of magnitude larger than those of $LnFeAsO$ [27, 28, 29]. Secondly, in contrast to $LaNiAsO$, the resistivity in $CeNiAsO$ shows a hump around 100 K. This could be ascribed to the f-electron contribution via Kondo scattering between the localized $4f$ - and the conduction $3d$ -electrons. We subtract the resistivity of $LaNiAsO$ from $CeNiAsO$, and the difference is shown in the upper inset. A broad maximum at 92 K becomes obvious. Similar broad peak is also observed in temperature dependent thermopower $S(T)$. Such a phenomenon is a distinct feature in Kondo lattice system, and can be explained by the Kondo scattering from different CEF levels[30, 31]. However, we can not exclude the possibility of onset of coherent Kondo scattering, provided that both have a comparable temperature scale. Thirdly, when temperature decreases down to around 9.3 K, a pronounced drop is observed, which is reminiscent of the reduction of spin-flip scattering when Ce moments become AFM ordered. Such a drop in resistivity was also observed in previous report [17]. Moreover, as further cooled, a small kink emerges around 7.3 K. We associate this kink with the transformation of Ce magnetic structure proposed hereinbefore. Finally, while $LaNiAsO$ is a superconductor with $T_c \sim 2.75$ K [6], no SC in $CeNiAsO$ is observed down to 30 mK, implying the influence of Kondo coupling on the conduction carriers. A small residual resistivity of $\rho_0 = 0.24 \mu\Omega \cdot m$ is derived, which again ensures the high purity of the sample. It should be noted that both R_H and S are positive above 150 K, and become negative below 100 K, manifesting a multi-band nature of the system in which hole-type carrier dominates at high temperature while electron-type charge carrier becomes dominant at low temperature. Whether this change of carrier type is CEF effect related needs more investigations.

The result of specific heat measurement is shown in Fig. 5. For high temperature, $C(T)$ follows good Dulong-Petit law and saturates to the classical limit of $4 \times 3R \sim 100$ J/mol·K (data not shown here). Considering the contributions from the phonons and the Schottky anomaly, the specific heat can be written as:

$$C = \gamma_0 T + \beta T^3 + C_{Sch} \quad (1)$$

for temperatures below $\Theta_D/10$, where Θ_D is the Debye temperature, γ_0 and β are coefficients of the electron and phonon contributions, while C_{Sch} is the Schottky anomaly item. We first subtract the specific heat of $LaNiAsO$ from the total specific heat, based on the assumption that both of them have the similar phonon contribution, to estimate the contribution from $4f$ electrons in $CeNiAsO$, and the difference (C^{4f}) is shown in the inset of Fig.5(a). C^{4f}/T does not go to zero at higher temperature ($T > 30$ K), but shows a broad peak centering at 50 K. This broad peak should be attributed to the Schottky anomaly caused by the excitations between different CEF levels. A Schottky anomaly formula with three Kramers doublets (one doublet ground state and two excited doublets)[12, 32] is used to fit this broad peak, i.e.,

$$C_{Sch}(T) = \frac{R}{g_0 + g_1 \exp(-\Delta_1/T) + g_2 \exp(-\Delta_2/T)} \\ \times \{g_0 g_1 (\Delta_1/T)^2 \exp(-\Delta_1/T) + g_0 g_2 (\Delta_2/T)^2 \exp(-\Delta_2/T)\}$$

$$+ g_1 g_2 [(\Delta_2 - \Delta_1)/T]^2 \exp[-(\Delta_2 - \Delta_1)/T] \} \quad (2)$$

where $g_i = 2$ is the degeneracy of the i th doublet state, and Δ_i is the energy difference between ground state and the i th excited state. The obtained energy differences from the fitting are $\Delta_1 = 10.5$ meV (~ 120 K) and $\Delta_2 = 32.8$ meV (~ 380 K). This result is consistent with the slope change in $1/\chi(T)$, as well as the observed pronounced broad maximum observed in both $\rho_{Ce} - \rho_{La}$ and S . Due to the large Δ_2 , it is likely that the reduction of effective Ce moment is caused by the CEF effect. We then subtract the fitted Schottky anomaly item from the total specific heat, and the result shows a good linear dependence in the $(C - C_{Sch})/T - T^2$ plot (see the inset of Fig. 5(b)) for the temperatures below 30 K. The extrapolated Sommerfeld coefficient $\gamma_0 \sim 203$ mJ/mol·K², which is more than 40 times of that of LaNiAsO (see in Tab. 1), manifesting the correlated effect contributed from the Ce 4*f*-electrons. Although the phonon contribution and the CEF effect is hard to be removed completely, our analysis should provide a good estimation of the Sommerfeld coefficient of CeNiAsO. The linear fit also produces that $\beta = 0.2511$ mJ/mol·K⁴ and Debye temperature $\Theta_D = 314$ K, which indicates the above analysis is quite self-consistent. For $T < 10$ K, two λ -shaped peaks are observed on the C/T curve, implying two successive phase transitions. This can be further confirmed by the derivative of susceptibility ($Td\chi/dT$), the derivative of resistivity ($d\rho/dT$), the magnetoresistivity ($\rho_{5T} - \rho_0$), and the Hall coefficient (R_H) shown in Fig. 5(b,c). The excellent agreement among C/T , $d\rho/dT$ and $Td\chi/dT$ leads to a definition of two characteristic temperatures, i.e., $T_{N1} = 9.3$ K and $T_{N2} = 7.3$ K. Actually, similar analysis has been widely applied in other nickel containing compounds, e.g., CeNiGe₃ [33] and $LnNi_2B_2C$ [34]. Note that the magnetic entropy gain derived by integrating C^{4f}/T over temperature reaches 70% of $R\ln 2$ at 10 K, and recovers the full doublet ground state ($R\ln 2$) at 30 K. All these indicate that both specific heat peaks are due to Ce-4*f* electrons related magnetic transitions, though the ordered moment is partially screened by the Kondo coupling in the ground state doublet. The Kondo scale is estimated to be $T_K \sim 15$ K by the entropy. A ratio of $T_K/T_{N1} \sim 1$ can also be obtained by judging from the specific heat jump $\Delta(C^{4f} - C_{Sch})$ at T_{N1} [35], thus it is reasonable that the Kondo scale $T_K \sim 15$ K. We propose that the transition at 9.3 K is originated from the Ce-AFM transition based on the magnetization measurement. We also notice that the similar phenomenon was also found in other Ce-based Kondo lattice compounds such as CeCu₂(Si_{1-x}Ge_x)₂, where the two peaks were explained by two incipient instabilities in the magnetic structure of pure CeCu₂Ge₂ [36, 37]: the first one at a higher temperature, related to a reorientation of the moments, and a second one at lower temperature, related to a lock-in of the propagation vector.

Now we turn to discuss the possible magnetic configurations of CeNiAsO. First of all, we should emphasize that all the observed magnetism should arise from the Ce moments. The negative value of the Weiss temperature (θ_W) indicates that Ce moments are AFM correlated. The most simplified model involves the intra-layer and inter-layer magnetic interactions between the nearest neighbor Ce moments, denoted by $J^{intra} = J_0 + J_{RKKY}^{intra}$ and $J^{inter} = J_{RKKY}^{inter}$, respectively. Where, J_0 is the superexchange

interaction via O^{2-} and As^{3-} anions in the absence of $d-f$ coupling [38], while J_{RKKY}^{intra} and J_{RKKY}^{inter} are the Ruderman-Kittel-Kasuya-Yosida (RKKY) interactions mediated by conduction electrons via $d-f$ coupling. Generally, J_0 is always negative ($J_0 < 0$) and favors AFM ordered ground state[38], while J_{RKKY}^{intra} and J_{RKKY}^{inter} are functions of Kondo coupling (J_K) and density of state at Fermi energy(N_{E_F}) [39]. We can assume $J_{RKKY}^{inter} \sim J_{RKKY}^{intra} = J_{RKKY}$, since they have almost the same k_F and the same nearest neighbor distances [40]. J_{RKKY} may be either negative (antiferromagnetic) or positive (ferromagnetic) depends on $J_K N_{E_F}$, which may account for either a G-type or C-type magnetic order respectively when cooled down (see the lower inset of Fig. 1). Actually, the changes in the Hall coefficient and thermopower at low temperatures indeed imply a temperature-induced change, either quantitatively or qualitatively, in the either density or relaxation time of different types of charge carriers. Thus it is plausible that a sign change occurs in J_{RKKY} when temperature is lowered down to $7K \sim 9K$, resulting in the magnetic transition from the G-type to C-type magnetic configuration within the Ce-AFM phase. This scenario provides a possible explanation on the two magnetic phase transitions, and it is consistent with the drop in the magnetic susceptibility ($\chi(T)$) in the G-type state and then an upturn as it enters C-type state at $T < T_{N2}$. Further experimental studies on the single crystalline sample of CeNiAsO and neutron diffraction measurement are necessary to testify this scenario.

Finally, it is interesting to compare CeNiAsO with its neighbors, CeFeAsO and CeCoAsO. Previous first principles calculation on LaTAsO [21] suggested that Fe and Co ions show SDW-like and FM instabilities at low temperatures respectively, while Ni ions display nonmagnetic behavior. For CeTAsO, Fe ions in CeFeAsO indeed show SDW-like AFM instability and Co ions in CeCoAsO are FM ordered[14, 15], meanwhile neither local magnetic moment nor long range magnetic order of Ni ions is observed in CeNiAsO. However, this does not mean that the Kondo coupling between Ce moment and conduction carriers in the NiAs layer is weaker than that in the FeAs layer. The situation could be totally on the contrary. We expect the Ce-4*f* level is much closer to the conduction band in CeNiAsO than those in CeFeAsO and CeCoAsO. Thus an enhanced hybridization between 4*f*- and 3*d*-electrons is possible in CeNiAsO due to the smaller *c*-axis lattice constant (see Tab. 1), as evidenced by the moderately large Sommerfeld coefficient and the absence of SC.

4. Conclusion

To summarize, the magnetic properties and specific heat of poly-crystalline CeNiAsO sample with high purity have been studied. Although CeNiAsO is much more metallic compared to its neighbor CeFeAsO, no superconductivity is observed down to 30 mK. Two successive antiferromagnetic transitions of Ce 4*f* electrons are observed. We propose that the Ce moments could align in G-type AFM at $T_{N1}=9.3$ K first, and then modify into C-type at a lower temperature $T_{N2}=7.3$ K. Regarding to the large Sommerfeld coefficient of about 203 mJ/mol·K², CeNiAsO represents a new example of AFM dense

Kondo lattice with Kondo scale $T_K \sim 15$ K in a wide class of the rare earth pnictides of the ZrCuSiAs-type [41]. A strong hybridization between 4*f*- and 3*d*-electrons is proposed and its influence on the ground state is discussed.

Acknowledgments

The authors would like to thank Qimiao Si, Huiqiu Yuan and Shuang Jia for helpful discussion. This work is supported by the National Science Foundation of China (Grant Nos 10634030 and 10931160425), the Fundamental Research Funds for the Central Universities of China (Program No. 2010QNA3026), and the National Basic Research Program of China (Grant Nos. 2007CB925001 and 2010CB923003).

References and Notes

- [1] Kamihara Y, Watanabe T, Hirano M and Hosono H 2006 *J. Am. Chem. Soc.* **130** 3296
- [2] Chen X H, Wu T, Wu G, Liu R H, Chen H and Fang D F 2008 *Nature (London)* **453** 761
- [3] Chen G F, Li Z, Wu D, Li G, Hu W Z, Dong J, Zheng P, Luo J L and Wang N L 2008 *Phys. Rev. Lett.* **100** 247002
- [4] Wen H H, Mu G, Fang L, Yang H and Zhu X 2008 *EPL* **82** 17009
- [5] Watanabe T, Yanagi H, Kamihara Y, Kamiyaa T, Hirano M and Hideo Hosono H 2008 *J. Solid State Chem.* **181** 2117
- [6] Li Z, Chen G, Dong J, Li G, Hu W, Wu D, Su S, Zheng P, Xiang T, Wang N and Luo J 2008 *Phys. Rev. B* **78** 060504(R)
- [7] Ren Z, Che G, Dong X, Yang J, Lu W, Yi W, Shen X, Li Z, Sun L, Zhou F and Z. Zhao 2008 *EPL* **83** 17002
- [8] Wang C, Li L, Chi S, Zhu Z, Ren Z, Li Y, Wang Y, Lin X, Luo Y, Xu X, Cao G and Xu Z 2008 *EPL* **83** 67006
- [9] Zhao J, Huang Q, de la Cruz C, Li S, Lynn J W, Chen Y, Green M A, Chen G F, Li G, Li Z, Luo J L, Wang N L and Dai P 2008 *Nature Materials* **7** 953
- [10] Brüning E M, Krellner C, Baenitz M, Jesche A, Steglich F and Geibel C 2008 *Phys. Rev. Lett.* **101** 117206
- [11] Luo Y, Li Y, Jiang S, Dai J, Cao G and Xu Z 2010 *Phys. Rev. B* **81** 134422
- [12] Krellner C, Kini N S, Brüning E M, Koch K, Rosner H, Nicklas M, Baenitz M and Geibel C 2007 *Phys. Rev. B* **76** 104418
- [13] Krellner C, Burkhardt U and Geibel C 2009 *Physica B* **404** 3206
- [14] Ohta H and Yoshimura K 2009 *Phys. Rev. B* **80** 184409
- [15] Sarkar B, Jesche A, Krellner C, Baenitz M and Geibel C, *Preprint* arXiv: 1006.5904 (2010)
- [16] Cao G, Jiang S, Lin X, Wang C, Li Y, Ren Z, Tao Q, Feng C, Dai J, Xu Z and Zhang F C 2009 *Phys. Rev. B* **79** 174505
- [17] Chen G F, Li Z, Wu D, Dong J, Li G, Hu W Z, Zheng P, Luo J L and Wang N L 2008 *Chin. Phys. Lett.* **25** 2235
- [18] Blanchard P E R, Cavell R G and Mar A 2010 *J. Solid State Chem.* **183** 1477
- [19] Izumi F and Ikeda T 2000 *Mater. Sci. Forum* **198** 321
- [20] Jiang S, Wang C, He M, Yu J, Tao Q, Dai J H, Xu Z A and Cao G H 2010 *Physica C* **470** S456
- [21] Xu G, Ming W, Yao Y, Dai X, Zhang S C and Fang Z 2008 *EPL*, **82** 67002
- [22] McQueen T M, Klimczuk T, Williams A J, Huang Q and Cava R J 2009 *Phys. Rev. B* **79** 172502
- [23] Ronning F, Bauer E D, Park T, Kurita N, Klimczuk T, Movshovich R, Sefat A S, Mandrus D and Thompson J D 2009 *Preprint* arXiv: 0902.4423
- [24] Beche E, Charvin P, Perarnau D, Abanades S and Flamant G 2008 *Surf. Interface Anal.* **40** 264

- [25] Ślebarski A, Radłowska M, Zygmunt A and Jezierski A 2002 *Phys. Rev. B* **65** 205110
- [26] Suga S, Takeda M, Mori Y, Shino N, Imada S and Kitazawa H 1993 *Physica B* **186-188** 63
- [27] McGuire M A, Hermann R P, Sefat A S, Sales B C, Jin R, Mandrus D, Grandjean F and Long G J 2009 *New J. Phys.* **11** 025011
- [28] Tao Q, Zhu Z, Lin X, Cao G, Xu Z, Chen G, Luo J and Wang N 2010 *J. Phys.: Condens. Matter* **22** 072201
- [29] Ishida S, Nakajima M, Tomioka Y, T. Ito T, Miyazawa K, Kito H, H. Lee C H, Ishikado M, Shamoto S, Iyo A, Eisaki H, Kojima K M and Uchida S 2010 *Phys. Rev. B* **81** 094515
- [30] Amato A, Jaccard D, Sierro J, Haen P, Lejay P and Flouquet J 1989 *J. Low Temp. Phys.* **77** 195
- [31] Zlatić V and Monnier R 2005 *Phys. Rev. B* **71** 165109
- [32] Chi S, Adroja D T, Guidi T, Bewley R, Li S, Zhao J, Lynn J W, Brown C M, Qiu Y, Chen G F, Luo J L, Wang N L and Dai P 2008 *Phys. Rev. Lett.* **101** 217002
- [33] Mun E D, Bud'ko S L, Kreyssig A, Canfield P C 2010 *Phys. Rev. B* **82** 054424
- [34] Ribeiro R A, Bud'ko S L and Canfield P C 2003 *J. Magn. Magn. Mater.* **267** 216
- [35] Besnus M J, Braghda A, Hamdaoui N and Meyer A 1992 *J. Magn. Magn. Mater.* **104** 1385
- [36] Trovarelli O, M. Weiden M, Müller-Reisener R, Gómez-Berisso M, Gegenwart P, Deppe M, Geibel C, Sereni J G, Steglich F 1997 *Phys. Rev. B* **56** 678
- [37] Hossain Z, Geibel C, Yuan H Q and Sparn G 2003 *J. Phys.: Condens. Matter* **15** 3307
- [38] Dai J, Zhu J X and Si Q 2009 *Phys. Rev. B* **80** 020505(R)
- [39] Doniach S 1977 *Physica B* **91** 231
- [40] We argue that J_{RKKY} depends on the Ce-Fe-Ce distance, thus inter-layer and intra-layer RKKY interactions have almost the same Ce-Fe-Ce distances.
- [41] Pottgen R and Johrendt D 2008 *Z. Naturforsch. B* **63** 1135

Table 1. Comparison among CeFeAsO, CeNiAsO and LaNiAsO. Atomic positions: Ln ($1/4, 1/4, z_{Ln}$), T ($3/4, 1/4, 1/2$), As ($1/4, 1/4, z_{As}$), O ($3/4, 1/4, 0$). Some data of CeFeAsO and LaNiAsO are taken from Ref.[11, 27, 5, 28].

$LnTAsO$	CeFeAsO	CeNiAsO	LaNiAsO
a (Å)	4.0002	4.0767	4.1231
c (Å)	8.6412	8.1015	8.1885
z_{Ln}	0.1411	0.1465	0.1470
z_{As}	0.6547	0.6434	0.6368
d_{TAs} (Å)	2.6736	2.3235	2.2404
$\theta_{As-T-As}$ ($^\circ$)	112.5	120.6	123.0
R_{wp}	11.96%	8.11%	7.52%
R_p	8.16%	5.73%	-
χ^2	1.12	0.88	2.02
$\rho(300K)$ ($\mu\Omega\cdot m$)	305.8	3.9	3.1
$R_H(300K)$ ($10^{-4}cm^3/C$)	<0	0.68	-1.0
$S(300 K)$ ($\mu V/K$)	-7.2	2.9	0.62
γ_0 (mJ/mol $\cdot K^2$)	~ 59	~ 203	~ 5

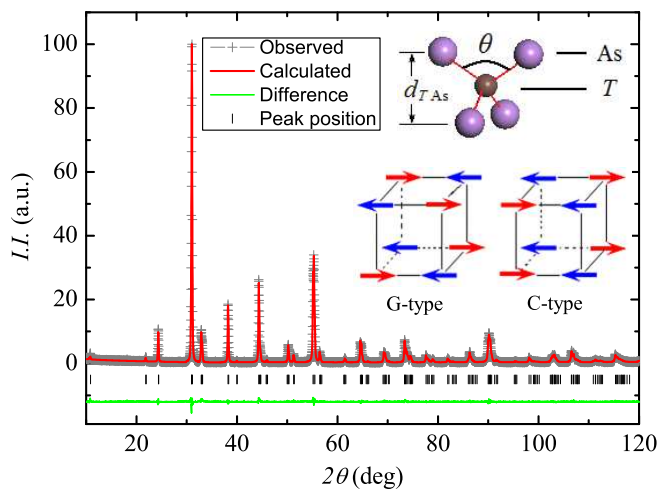


Figure 1. (Color Online) Rietveld refinement of CeNiAsO XRD pattern. Upper inset shows the schematic diagram of TAs layer. The sketches of the proposed G type and C type magnetic structures are also shown in the lower inset.

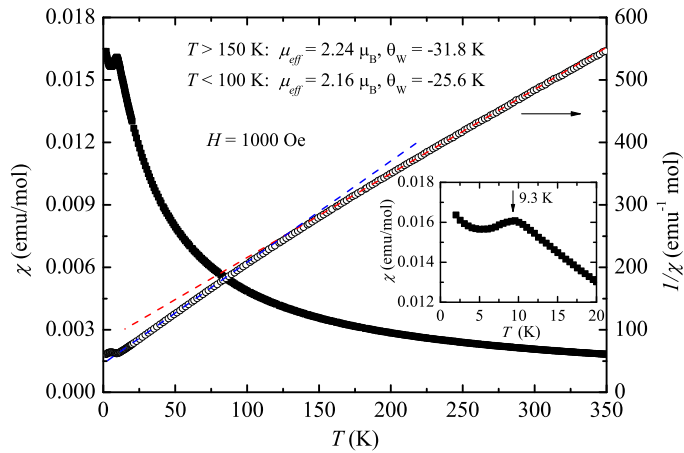


Figure 2. (Color Online) Temperature dependence of magnetic susceptibility of CeNiAsO. The two dashed lines signify Curie-Weiss fit for $T > 150$ K (red) and $T < 100$ K (blue), respectively. Inset: Enlarged plot of $\chi(T)$ at $T < 20$ K.

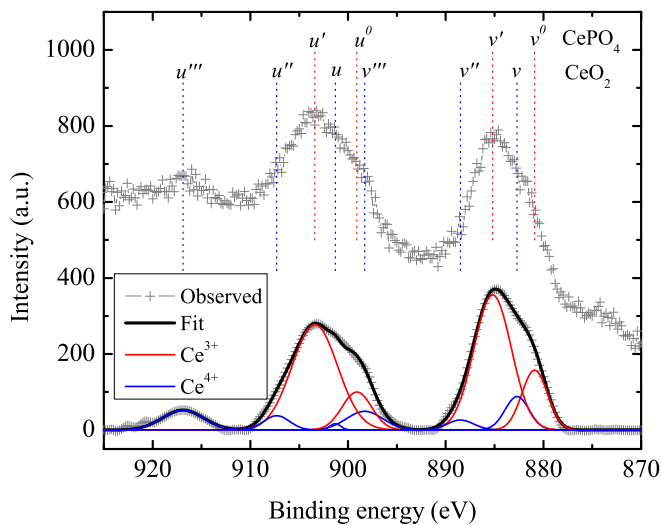


Figure 3. (Color Online) Room temperature XPS spectrum. Ce(III) = $v^0 + v' + u^0 + u'$, and Ce(IV) = $v + v'' + v''' + u + u'' + u'''$. On the assumption of intermediate valence of Ce, the XPS spectrum was fitted to a combination of ten Gaussian functions.

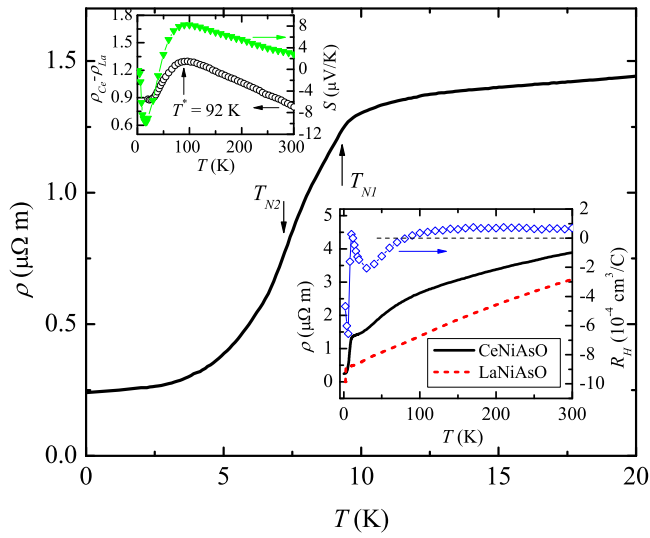


Figure 4. (Color Online) Electrical transport properties of CeNiAsO. Main frame: resistivity at low temperature ($T < 20$ K), with two arrows signifying the two magnetic transitions at 9.3 K and 7.3 K. Lower inset: temperature dependent resistivity of LaNiAsO and CeNiAsO, and Hall coefficient of CeNiAsO. Upper inset: The difference of resistivity between CeNiAsO and LaNiAsO, $\rho_{Ce} - \rho_{La}$, as well as the thermopower S .

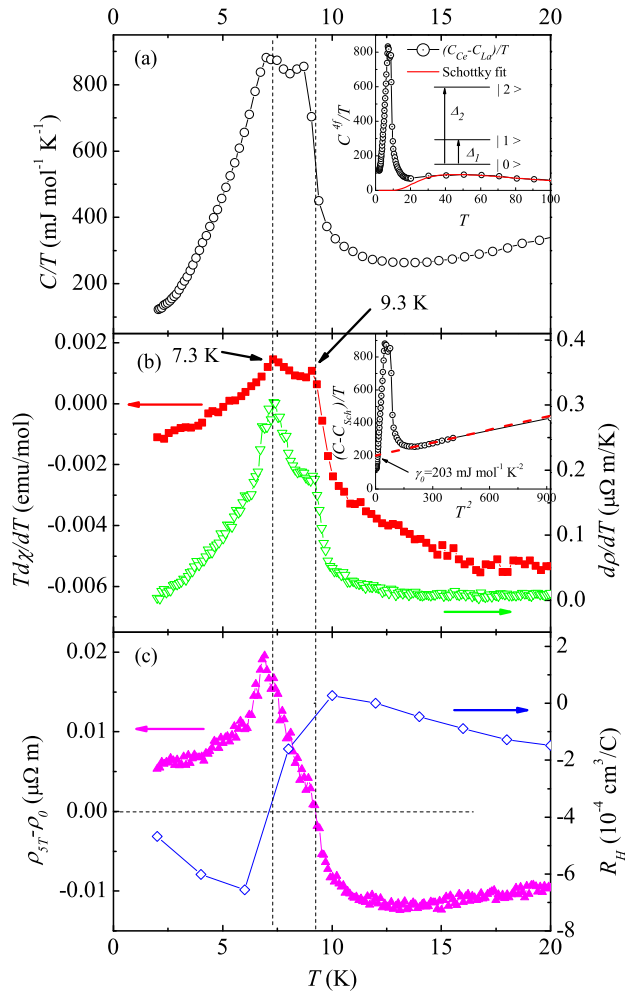


Figure 5. (Color Online) Evidences for the two magnetic transitions below 10 K, from (a), specific heat; (b), derivative susceptibility ($Td\chi/dT$) and derivative resistivity ($d\rho/dT$); (c), magnetoresistivity ($\rho_{5T} - \rho_0$) and Hall coefficient (R_H). Inset of (a) displays the Schottky anomaly fit of C^{Af}/T . Inset of (b) shows γ_0 derived from extrapolating $(C - C_{Sch})/T - T^2$ plot to zero limit.